Hadronic Regge trajectories: Problems and approaches

A. Inopin
Virtual Teacher Ltd., Vancouver, Canada

G. S. Sharov
Tver State University, Sadovyj per., 35, 170002 Tver, Russia
(Received 26 July 1999; published 7 February 2001)

We scrutinize hadronic Regge trajectories in the framework of two different models — string and potential. Our results are compared with a broad spectrum of existing theoretical quark models and experimental data from PDG98. It was recognized that Regge trajectories for mesons and baryons deviate from straight and parallel lines in general in the current resonance region both experimentally and theoretically. They very often have appreciable curvature, which is flavor dependent. For a set of baryon Regge trajectories this fact is well described in the considered potential model. The standard string models predict linear trajectories at high angular momenta J with some form of nonlinearity at low J. This model is also adequate for the majority of orbitally excited hadron states.

DOI: 10.1103/PhysRevD.63.054023 PACS number(s): 12.40.Nn, 14.20.−c, 14.40.−n

INTRODUCTION

In the past few years Regge trajectories (RT) have attracted the interest of many authors, who build quark models of baryons, mesons, glueballs and hybrids [1–19]. Quite a number of approaches have been used to attack this problem: the WKB approach [1,2], the Wilson loop model [3,4], the $\hbar$-expansion technique [5], the q-deformed algebra approach [6], the $1/N_c$ approach [7], the spectrum generating algebra (SGA) model [8], the Filipponi-Pancheri-Srivastava (FPS) model [9], the nonrelativistic quark model (NRQM) [10], string models [11–15], the extended covariant oscillator quark model for glueballs [16], N/D method [17], and others.

Probably, the most interesting questions which are under investigation are the following. (a) Are the RT really straight lines in the entire energy interval, or is this only true asymptotically? (b) Do the trajectories for mesons, baryons, glueballs and hybrids have the same slope? (c) What is the flavor dependence of RT? (d) What is the intrinsic connection between kinematics, the type of the potential, and the straightness of RT? (e) When does the asymptotic regime ($J=?$) really start for baryons, mesons, glueballs, hybrids for both parent and daughter (ancestor) trajectories? (f) What is the dependence of the character of RT on the scalar or vector structure of the confinement potential?

Different groups pursued variety of models and different aspects of this problem. It was established long ago, that the experimental RT for N, Δ baryons are not strictly straight lines [18]. The authors of this seminal review and Hendry in Ref. [19] considered the facts of nonlinear behavior of the RT in mass squared. Rather, as Hendry concludes, baryon resonances seem more linear as a function of c.m. momentum.

In this paper we will consider this problem from the point of view of two different models — potential [10] (Secs. I,II) and string [15] (Sec. III). Then we will contrast our results with broad spectrum of existing theoretical models and experimental data for different flavors and draw the conclusions about deviation of both experimental and theoretical RT from linearity and description of experimental data by various models.

I. REGGE TRAJECTORIES IN THE POTENTIAL QUARK MODEL

In our recent series of papers [10], based on Hamiltonian (1) and the method of hyperspherical functions (HF) [20], a description of N, Δ, Ω resonance spectra and partial widths was given

$$H=H_0+H_{\rm hyp},$$

$$H_0=\sum_{i=1}^{3} m_i+\sum_{i=1}^{3}\frac{\boldsymbol{P}_i^2}{2m_i}-\frac{2}{3}\sum_{i<j}\left(\frac{\alpha_s}{r_{ij}}-br_{ij}\right)+V_0,$$

$$H_{\rm hyp}=\frac{2}{3}\sum_{i<j}\frac{\pi C_\alpha}{m_i^2}\left(1+\frac{8}{3}(\boldsymbol{s}_i\boldsymbol{s}_j)\right)\delta(\boldsymbol{r}_{ij})+\sum_{i<j}\frac{2C_t}{3m_im_jr_{ij}^3}\left[3\frac{(\boldsymbol{s}_i\boldsymbol{r}_{ij})(\boldsymbol{s}_j\boldsymbol{r}_{ij})}{r_{ij}^2}-\boldsymbol{s}_i\boldsymbol{s}_j\right]. \quad (1)$$

Following Ref. [21], we introduce the constants α_s, C_α, and C_t, which determine the strength of the Coulomb, contact and tensor potentials, respectively. The use of the Hamiltonian (1) allows us to obtain better agreement with experiment for resonances of positive and negative parity, and also to describe resonances with both large J and M, and with small J and M.

We showed [10] that it was appropriate for such a description to take advantage of the concept of yrast states and yrast lines from the theory of atomic nuclei rotational spectra, as well as to make use of the concept of RT. One of the main results was that both theoretical and experimental spectra are *nonlinear* trajectories in Chew-Frautschi plots

TABLE I. Masses of the predicted N, Δ resonances in the model [10].

$N\ 11/2^+$ (2.39)	$N\ 13/2^-$ (2.90)	$N\ 15/2^+$ (3.00)
$N\ 17/2^-$ (3.45)	$N\ 19/2^+$ (3.45)	$N\ 21/2^-$ (3.95)
$\Delta\ 15/2^-$ (3.48)	$\Delta\ 17/2^+$ (3.49)	$\Delta\ 19/2^-$ (4.00)

throughout the experimental region. Our model predicts a whole series of high-lying N, Δ resonances, represented in Table I.

The present paper generalizes the model [10] to u, d, s, c, b flavors (it is impossible to create top baryons and mesons) and a wider range of angular momenta $L=0-20$. We obtain the spectra of baryon resonances in the same way as in [10], by solving Schrödinger equation (SE) with the HF method.

When the hadron wave function (WF) is expanded in the HF basis and substituted in the SE, one generally finds an infinite system of differential equations for the radial WF (RWF). However, as was shown in Ref. [20] for a system of identical u, d quarks, the coupling of channels is weak, therefore it is sufficient to include only several terms in K, grand orbital momentum, in the WF expansion. With increasing excitation energy, the contribution of $H_{\rm hyp}$ vanishes, hence the coupling of channels in general can be neglected. On the other hand, as we will consider only symmetric baryons with increasing quark mass (u, s, c, b), the abovementioned arguments will apply even more strongly.

Now, let us introduce Jacobi and hyperspherical coordinates for a three-body problem. The Jacobi coordinates are defined as usual (please see Ref. [10] for all the details)

$$\boldsymbol{R}=(\boldsymbol{r}_1+\boldsymbol{r}_2+\boldsymbol{r}_3)/3, \quad \boldsymbol{\eta}=(\boldsymbol{r}_1-\boldsymbol{r}_2)/\sqrt{2},$$

$$\boldsymbol{\xi}=(\sqrt{2/3})[(\boldsymbol{r}_1+\boldsymbol{r}_2)/2-\boldsymbol{r}_3]. \tag{2}$$

The hyperspherical angle θ and radius ρ are defined as follows:

$$\eta=\rho\cos\theta, \quad \xi=\rho\sin\theta, \quad 0<\theta<\pi/2,$$

$$\rho=(\eta^2+\xi^2)^{1/2}, \quad 0<\rho<\infty. \tag{3}$$

So, our WF and q-q potentials will depend on new variables $\boldsymbol{\eta}$ and $\boldsymbol{\xi}$.

We will work in the hypercentral approximation (HCA), where only that part of the interaction which is invariant under rotation in six-dimensional space (ρ,Ω_5) is taken into account. Because in HCA baryons are pure *rotational* states in six-dimensional space, and because a very soft potential is used in our model, no strong correlations generating a so-called quark-diquark state can occur. So, we will neglect the θ dependence of our q-q potential. The introduction of θ dependence in the potential mixes the states belonging to one value of L, and slightly shifts their positions in the baryonic mass spectrum. As was proved by Richard [20], the most commonly used potentials in hadron spectroscopy (including ours) are very close to hypercentral.

TABLE II. Input parameters in the model [10].

$\alpha_s=C_\alpha=1$	$C_t=0.2$	$b=350$ MeV/fm
$V_0=-513$ MeV	$m_u=330$ MeV	$m_d=330$ MeV
$m_s=607$ MeV	$m_c=1500$ MeV	$m_b=5170$ MeV

II. MASS SPECTRA AND RT IN THE POTENTIAL QUARK MODEL

Now let us discuss our results for mass spectra and RT of baryons. The method of numerical solution of the SE was described in detail in Ref. [10], but we will briefly recapitulate it here. The system of differential equations (SDE) was reduced to a system of first-order differential equations, which we integrated by determining a full set of Cauchy solutions. We then constructed the required solution by imposing the following boundary conditions on the RWF: $F_i(\rho=0)=0$ and $F_i(\rho=R_\infty)=0$. The eigenvalues (EV) were determined by zeroing the determinant constructed from the fundamental system of solutions for SDE. For the parameter R_∞ we always choose a much larger value than the radius of the corresponding excited state $\langle\rho\rangle_i$, which grows with L and N_r (the radial quantum number). We always choose R_∞ such that if we take $R_\infty=2R_\infty$, then the corresponding EV of any excited state will not change more than 1%. We use in our computation the following set of parameters (Table II). With this input we have calculated the mass spectra, RT, mean radii $\langle\rho\rangle_i$ and slopes for u, d, s, c, b flavors, $N_r=0,1,2$, and momenta range $L=0-20$.

We note that the solution of the SE in the single-channel approximation with the centrifugal potential $V_c=(K+3/2)(K+5/2)/(2m\rho^2)$ is equivalent from the mathematical point of view to the Davydov-Chaban model [22], in which the rotational spectrum of a nonspherical nucleus with variable moment of inertia is calculated. Because the moment of inertia is not constant but varies linearly with the angular momentum J of the nucleus, the rotational spectrum, instead of the quadratic behavior $J(J+1)$, it would have for a constant moment of inertia, approaches one linear in J.

Approximately the same thing happens with the hadron: for large excitation energies the spectrum becomes linear in J, and the hadron becomes a strongly extended system along its symmetry axis. This should lead to a linear nature of the baryonic mass spectra along yrast lines. Our predictions are in accord with findings by Hey [18] and Hendry [19].

Let us start a detailed, sector by sector comparison of our results for different flavors. Note that RT $[M^2=M^2(J)]$ for baryons have different types of curvatures: some are convex; others are concave functions of J (see Fig. 1). The u-d (N, Δ) trajectories are concave for $N_r=0,1,2$, whereas strange (sss) RT for $N_r=0,1,2$ are ''stereotypical'' — they are nearly straight lines with slowly varying slopes α' (Fig. 2). Charmed (ccc) and bottom (bbb) trajectories are convex for $N_r=0,1,2$.

When we analyze the mass spectra $M=M(J)$ for u-d, s, c, b baryons, they are all convex functions of J, with a rather complex dependence on m_q (flavor) and N_r. If we fix m_q and look at the Chew-Frautschi plot for $N_r=0,1,2$, we can see that these three curves generally are nonparallel (Fig. 1),

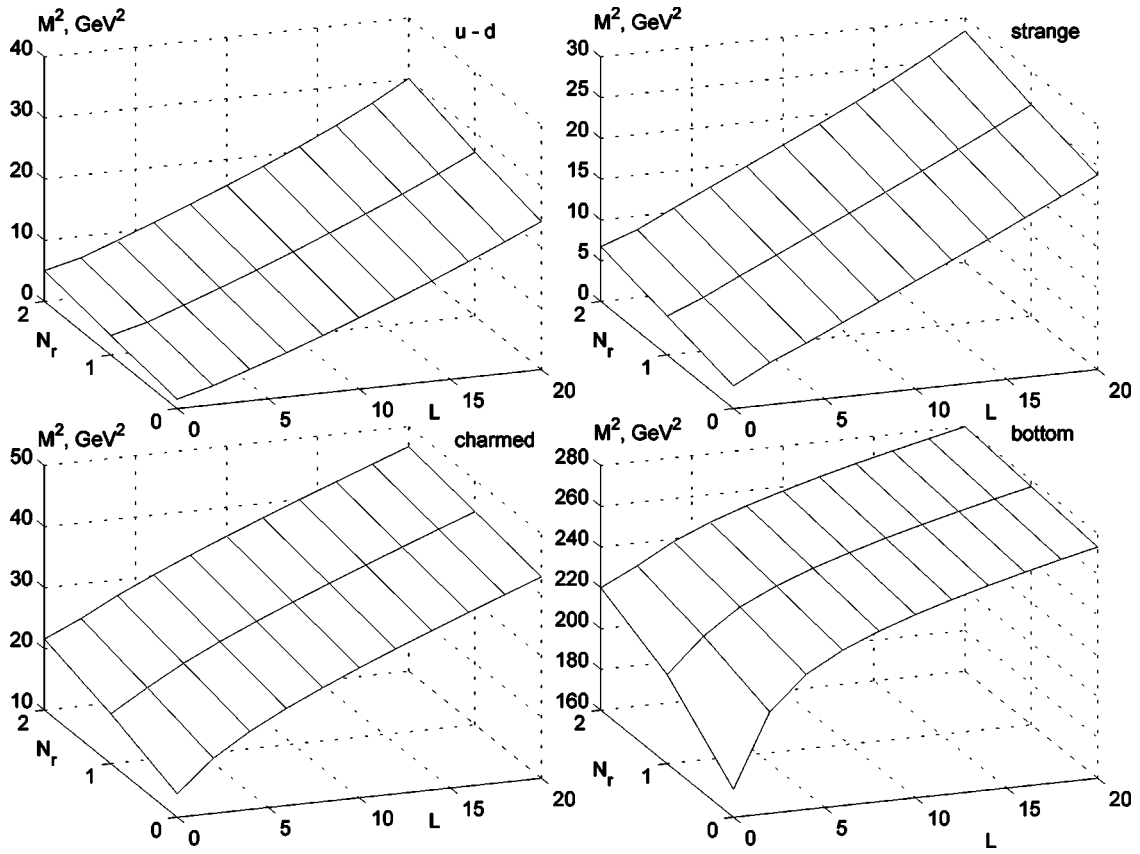

FIG. 1. Parent and two daughters RT in the potential quark model.

that strongly contradicts the conventional picture of the parallel RT. It is noteworthy that Olsson *et al.* [13] recently examined the meson sector, using a relativistic flux-tube model, and noticed nonlinearity of RT at low angular momenta J. But it remains unclear whether their model accounts adequately for physical observables, because it describes a very limited number of states in the mesonic sector.

Slopes for the u-d family start above 1 GeV^{-2}, with the largest value for $N_r=2$; the curves decrease almost monotonically with changing the rate of decreasing near $L=4$, for $N_r=0,1,2$ (see Fig. 2).

Slopes for the s family differ from all the other cases, because they are rather weak functions of L. Slopes for daughters $N_r=1,2$ start just above unity, then slowly decrease to 0.87 and 0.78 GeV^{-2}, respectively, whereas the parent slope fluctuates slightly over the interval, spanning the range 0.97–0.91 GeV^{-2} (see Fig. 2).

Slopes for the charm family are highly nonlinear functions of L. The $N_r=0,1$, slopes increase monotonically, starting from 0.39 and 0.55 GeV^{-2} and approaching 0.889 and 0.893 GeV^{-2}, respectively. The $N_r=2$ slope has a dip at $L=4$, and grows continuously, reaching 0.897 GeV^{-2}. These values are almost *identical* to Olsson's results for mesons for asymptotic L [13].

Bottom baryon slopes differ *sharply* from the u-d-s-c sector, first, by their small magnitude, and second, by the significant increase of the slopes along the trajectory (the B slopes increase by about an order of magnitude, from 0.055 to 0.504 GeV^{-2}). Daughter slopes for $N_r=2$ fluctuate, but still increase with L.

For convenience, we present the set of median values $\langle\alpha'\rangle_i$ for the whole flavor multiplet (see Table III). It is interesting to note that the median values of α_i' are almost independent of N_r for the u-d and s families.

The expectation values of the hyperradius $\langle\rho\rangle_i$ are basically smooth increasing functions of L and N_r, and decreasing functions of m_q.

We proved that the slope of the trajectories decreases with increasing quark mass in the mass region of the *lowest* excitations. This is due to the contribution of the color Coulomb interaction that increases with mass and results in a *curvature* of RT near the ground state. In the asymptotic regime the trajectories for all flavors are linear and have the same slope $\alpha'\simeq 0.9$ GeV^{-2}.

After careful numerical evaluation of baryon and meson spectra for all flavors we have shown that the point of establishment of linear RT depends on the exponent ν in the

TABLE III. Median values $\langle\alpha'\rangle_i$ for trajectories with $N_r=0,1,2$.

N_r	Up-down	Strange	Charm	Bottom
0	0.90	0.95	0.73	0.31
1	0.87	0.95	0.77	0.34
2	0.84	0.94	0.81	0.37

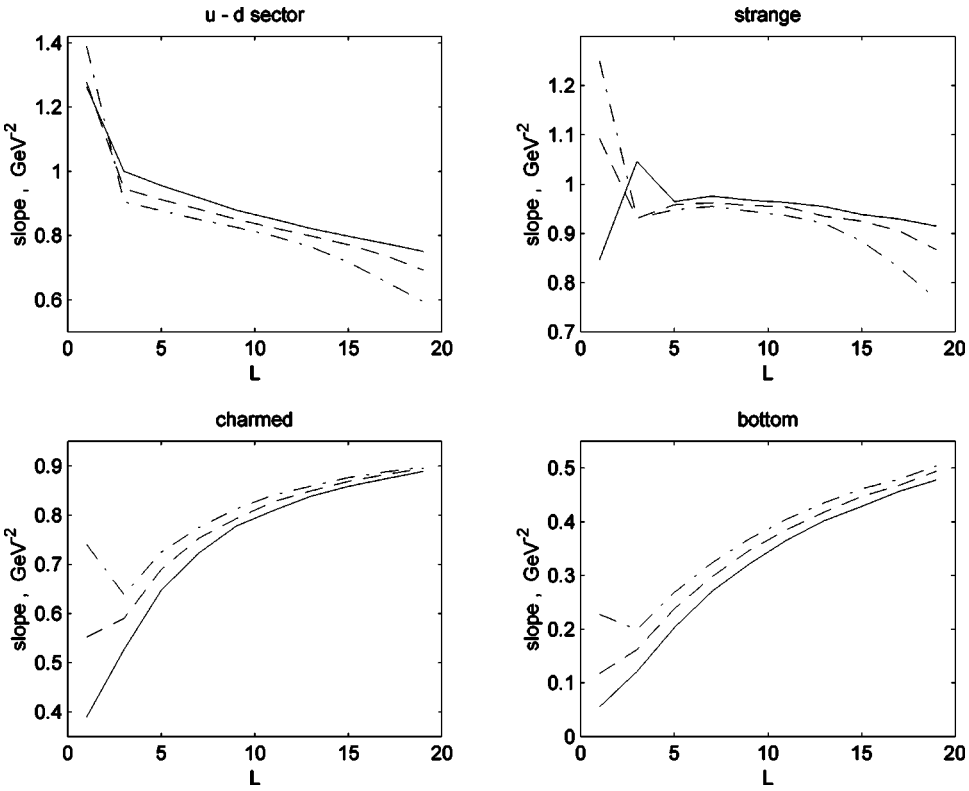

FIG. 2. Slopes for parent and two daughters RT in the potential quark model (solid lines: parent RT; dashed: $N_r=1$ RT; dashed-dotted: $N_r=2$ RT).

power law potential in Hamiltonian (1), and occurs at larger L with larger ν. The linear regime started only from $L>20$ for the oscillator confinement ($\nu=2$) and it started from $L>18$ for the linear confinement ($\nu=1$).

We proved that for mesons linear RT is established earlier than for baryons as a function of L. The reason lies in centrifugal energy term, which has $L(L+1)$ dependence for mesons and $(L+3/2)(L+5/2)$ dependence for baryons. As we see, three-dimensional corrections to $L(L+1)$-law are important for baryons.

III. STRING MODELS

The string models are widely used for describing orbitally excited hadron states by virtue of some remarkable features: (a) the direct analogy between the string with linearly growing energy and the QCD confinement mechanism of connecting quarks (antiquarks) by the gluon field tube [23]; (b) the strings are relativistic by definition;[1] (c) the energy $E=M$ and the angular momentum J of a rotating open (massless) string are connected by the Nambu relation [24]

$$J=\alpha' M^2, \quad \alpha'=(2\pi\gamma)^{-1}, \tag{4}$$

where γ is the string tension. This fact allows us to apply the string models to describing the RT.

The massless string generates the strictly linear RT (4). But more realistic meson model of relativistic string with massive ends [11] results in the more complicated behavior of RT. For this model the relation (4) takes place only in the high-energy limit [11,12].

String models of baryon were suggested in four variants differing from each other in the topology of spatial junction of three massive points (quarks) by relativistic strings: (a) the quark-diquark model q-qq [12] (on the classical level it coincides with the mentioned meson model [11,23]); (b) the linear configuration q-q-q with quarks connected in series [15,25]; (c) the ''three-string'' model or Y configuration with three strings joined in the fourth massless point (junction) [26,27]; and (d) the ''triangle'' model or Δ configuration that could be regarded as a closed string carrying three pointlike masses [28,29].

The classical equations of motion and the boundary conditions on the quark[2] trajectories in these models are deduced by variation and minimization of action for each of mentioned string hadron models [11,15,23,28,30]. In particular, under the conditions of orthonormality (they may be obtained for all configurations [23,28]) the equations of motion become linear

$$\frac{\partial^2 X^\mu}{\partial\tau^2}-\frac{\partial^2 X^\mu}{\partial\sigma^2}=0, \tag{5}$$

and the boundary conditions take the simplest form

$$m_i\frac{d}{d\tau}\frac{V_i^\mu}{|V_i|}=F_i^\mu. \tag{6}$$

[1]The relativistic string dynamics results from the extremization of a world surface area swept by the string in Minkowski space.

[2]The term ''quark'' here is equivalent to ''material point.''

Here $x^\mu = X^\mu(\tau,\sigma)$ is the string world surface in d-dimensional Minkowski space, m_i are masses of the material points (quarks), $V_i^\mu = (d/d\tau)X^\mu[\tau,\sigma_i(\tau)]$ is the tangent vector to the ith quark trajectory $\sigma = \sigma_i(\tau)$; the tension forces $F_i^\mu = \pm \gamma Y_i^\mu|_{\sigma=\sigma_i}$ for a quark at an end of the string, but $F_i^\mu = \gamma Y_i^\mu|_{\sigma=\sigma_i+0} - \gamma Y_i^\mu|_{\sigma=\sigma_i-0}$ for a quark in the ''triangle'' model and for the middle quark in the q-q-q system [28], $Y_i^\mu = \partial_\sigma X^\mu + \sigma_i'(\tau)\partial_\tau X^\mu$. The derivatives of $X^\mu(\tau,\sigma)$ are not continuous at $\sigma = \sigma_i$ in general. Some additional closure conditions for the configurations Δ [28,29] and Y [26,27] (for the junction) are required.

The string models are successfully applied to describing the main or parent RT. For this RT, that is for the orbitally excited hadrons the rotational motions of all string configurations (flat uniform rotations of the system) are used [12,14,15,29]. The solution of this type satisfying Eq. (5), conditions (6), and describing the uniform rotation of the rectilinear string is well known for the meson string model [11,23] (or its equivalent q-qq model) and for the q-q-q baryon configuration. It may be represented as

$$X^0 \equiv t = \tau, \quad X^1 + iX^2 = \omega^{-1} \sin \omega\sigma \cdot e^{i\omega\tau}. \tag{7}$$

Here $X^1 \equiv x$, $X^2 \equiv y$, ω is the angular velocity, $\sigma \in [\sigma_1, \sigma_N]$, $\sigma_i = \text{const}$, $\sigma_1 < 0 < \sigma_N$, $N = 2$ for the meson.

For the linear q-q-q configuration here $N = 3$ and the middle quark is at rest at $\sigma = \sigma_2 = 0$. But this motion is unstable with respect to centrifugal moving away of the middle quark that results in the complicated quasiperiodical motion [25] but without transforming into the configuration q-qq. So the q-q-q system is probably applicable not to pure orbital excitations but to radial ones. The rotational motion of the ''three-string'' model with the junction at rest and with rectilinear string segments joined in a plane of rotation at the angles 120° [26,27] is described by the expression similar to Eq. (7).

For the meson string model and for the baryonic configurations q-qq ($N=2$), q-q-q, and Y ($N=3$) the energy $E \equiv M$ and the angular momentum J of the considered rotational motions are [11,12,15]

$$M = \sum_{i=1}^{N} \left[\frac{\gamma}{\omega} \arcsin v_i + \frac{m_i}{\sqrt{1-v_i^2}} \right] + \Delta M, \tag{8}$$

$$J = \sum_{i=1}^{N} \left[\frac{1}{2\omega} \left(\frac{\gamma}{\omega} \arcsin v_i + \frac{m_i v_i^2}{\sqrt{1-v_i^2}} \right) + s_i \right], \tag{9}$$

where $v_i = \sin|\omega\sigma_i| = \sqrt{(m_i\omega/2\gamma)^2 + 1} - m_i\omega/2\gamma$ are the velocities of moving quarks. The presence of quark spins with projections s_i ($\Sigma_{i=1}^N s_i = S$) is taken into account as the correction ΔM to the energy of the classic motion. In Refs. [12,15] this correction is due to the spin-orbit interaction (the spin-spin correction is assumed to be small in comparison with the spin-orbit one at high J).

Soloviev [14] considers the dynamics of rectilinear meson string with some form of spin terms in the action and obtains the expressions similar to Eqs. (8),(9) with $\Delta M = 0$, the substitution J by $\sqrt{J(J+1)}$ and $\Sigma_{i=1}^N s_i$ by the phenomenological parameter a_n. The values a_n (different for various RT) are calculated by fitting.

The rotational motions (uniform rotations about the system center of mass) for the ''triangle'' baryon model [15,28,29] may be presented in the form

$$X^0 = \tau - \frac{T}{D}\sigma, \quad X^1 + iX^2 = u(\sigma) \cdot e^{i\omega\tau}. \tag{10}$$

Here the values σ_i, $D = \sigma_3 - \sigma_0$, V_i^2, $\tau^* - \tau = T$ are the constants, $X^\mu(\tau,\sigma_0) = X^\mu(\tau^*,\sigma_3)$ is the closure condition, the complex function $u(\sigma) = A_i \cos\omega\sigma + B_i \sin\omega\sigma$, $\sigma \in [\sigma_i, \sigma_{i+1}]$ is continuous in $[\sigma_0, \sigma_3]$. Expression (10) is the solution of Eq. (5) and satisfies the orthonormality, closure, and boundary (6) conditions if six complex constants A_i, B_i and the parameters of the motion (10) σ_i, D, T, ω, v_i, m_i/γ are connected by a set of relations [15,29–31]. A string position for this state [a section $t = \text{const}$ of the surface (10)] is the closed curve composed of three segments of a hypocycloid.

The energy and the angular momentum of the state (10) are [28,29]

$$M = \gamma D \left(1 - \frac{T^2}{D^2} \right) + \sum_{i=1}^{3} \frac{m_i}{\sqrt{1-v_i^2}} + \Delta M,$$

$$J = \frac{1}{2\omega} \left[\gamma D \left(1 - \frac{T^2}{D^2} \right) + \sum_{i=1}^{3} \frac{m_i v_i^2}{\sqrt{1-v_i^2}} \right] + S,$$

where v_i are the quark velocities.

A set of topologically different configurations of the system is classified in Refs. [29,31]. It is described, in particular, by integer parameters n and k which are $n = \lim_{m_i \to 0} D/(\sigma_1 - \sigma_0)$, $k = n \lim_{m_i \to 0} T/D$. The states with $n=3$, $k=1$ (simple states [29,31]) are used below for describing the RT. It was shown in Ref. [32] that they are stable (unlike in the q-q-q case [25]), in particular, with respect to transformation into the ''q-qq'' state with $n=2$, $k=0$.

In the two variants of describing RT with the help of string models in Refs. [12] and [15] the spin-orbit correction to the energy

$$\Delta M_{SL} = \sum_i \beta(v_i)(\boldsymbol{\omega}\mathbf{s}_i) \tag{11}$$

were used in the two different forms. In Ref. [12] the expression $\beta(v_i) = -[(1-v_i^2)^{-1/2} - 1]$ is due to the Thomas precession of the quark spins. It is obtained under the assumption that in the quark rest frame the field is pure chromoelectric [12,33]. The alternative assumption about pure chromoelectric field in the rotational center rest frame results in $\beta(v_i) = 1 - (1-v_i^2)^{1/2}$ [15,33].

The ultrarelativistic asymptotic behavior of the dependence $J(M)$ for the q-qq or mesonic string with massive ends [11,34,35], Y and Δ configurations has the form

TABLE IV. Input parameters in the string model.

$\gamma=\gamma_{q-qq}=0.175$ GeV^2	$\gamma_Y=\frac{2}{3}\gamma$	$\gamma_\Delta=\frac{3}{8}\gamma$
$m_u=m_d=130$ MeV	$m_s=300$ MeV	$m_c=1600$ MeV

$$J\simeq\alpha' M^2-\nu M^{1/2}\sum_{i=1}^{N} m_i^{3/2}+\Delta J, \quad v_i\to 1, \tag{12}$$

where $\alpha'=(2\pi\gamma)^{-1}$ for the meson and q-qq models, $\alpha'=\frac{2}{3}(2\pi\gamma)^{-1}$ for Y and $\alpha'=n(n^2-k^2)^{-1}(2\pi\gamma)^{-1}$ for Δ (ν also different for these configurations [15,30]). The term ΔJ equals $\Delta J=\Sigma_{i=1}^{N} s_i[1-\beta(v_i)]$ for the spin-orbit correction (11) [15,30] and $\Delta J=a_n-1/2$ for the meson string model [14].

The Regge slope $\alpha'\simeq 0.9$ GeV^{-2} is close for mesons and baryons. So the effective value of string tension γ is to be different for the baryon models Y, ''triangle'' (simple states), and q-qq. The following values of the parameters are used here (for this values the baryon configurations q-qq, Y, and Δ result in very close RT).

In Refs. [12] the q-qq model with the values $m_{ud}=340$ MeV, $m_s=440$ MeV is used. But the Thomas precession term in Eq. (11) results in the strong dependence (from 220 to 550 MeV) of the diquark mass on the spin state. On the other hand in Ref. [14] the current quark masses are used for describing mesons.

In this paper we use the string models (q-qq, Y, and Δ for baryons) with the parameters in Table IV and the spin-orbit correction (11) with $\beta(v_i)=1-(1-v_i^2)^{1/2}$ for describing parent RT. The results for light baryons (N and Δ RT) are shown in Figs. 3–5. The particle data are taken from the PDG98 issue [36]. In Fig. 3 the N-baryon states with $J^P=1/2^+$, $3/2^-$, $5/2^+$, $7/2^-$, . . . , are placed and described by our two models as two different RT. The dotted line shows the potential model [10] predictions for the RT with positive parity $p1/2^+$, $N(1680)5/2^+$, . . . ; the dash-dotted line corresponds to the states with negative parity. The same notations are used in Figs. 4–8.

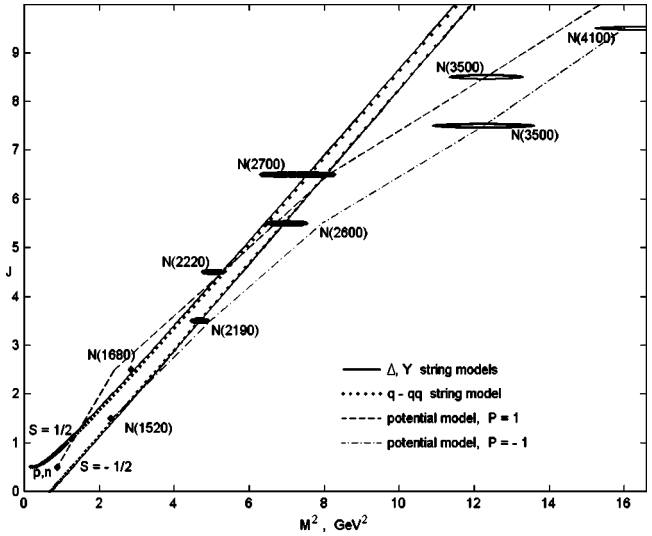

FIG. 3. RT for N baryons with $J^P=1/2^+,3/2^-,5/2^+,7/2^-,\ldots$.

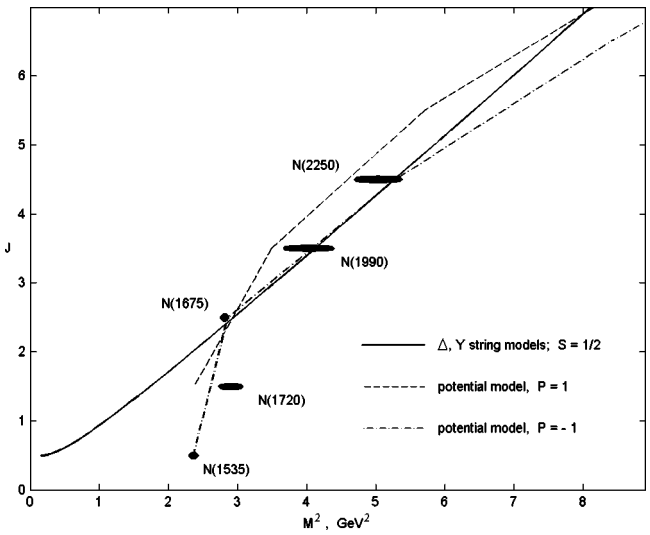

FIG. 4. RT for N baryons with $J^P=1/2^-,3/2^+,5/2^-,7/2^+,\ldots$.

The dependence $J=J(M^2)$ for the string models ''triangle'' and ''three-string'' is shown in Figs. 3–7 as solid lines (under the conditions in Table IV these curves practically coincide). Dots correspond to the q-qq model and they are very close to the previous curves. String hadron models [12–15] at the modern stage are (semi)classical and do not describe the isospin and parity. So in this paper we use only the spin projection $S=\Sigma s_i$ (here $J=L+S$) for modelling various RT. For example, in Fig. 3 the N states with positive and negative parity may be described as two different RT in all (potential and string) models. In the string models the spin states $S=1/2$ and $S=-1/2$ are used for these two RT — the curves $J=J(M^2)$ are close to rectilinear and fit the majority of states, except for the nucleon ($L=0$) and the states with $M>3000$ MeV which need confirmation [19] (they are omitted from the summary table [36]). But the latter baryons are described in the potential model [10] rather well.

For the Δ resonances in Fig. 5 a similar picture takes place. The states on the $\Delta(1232)$ trajectory with positive

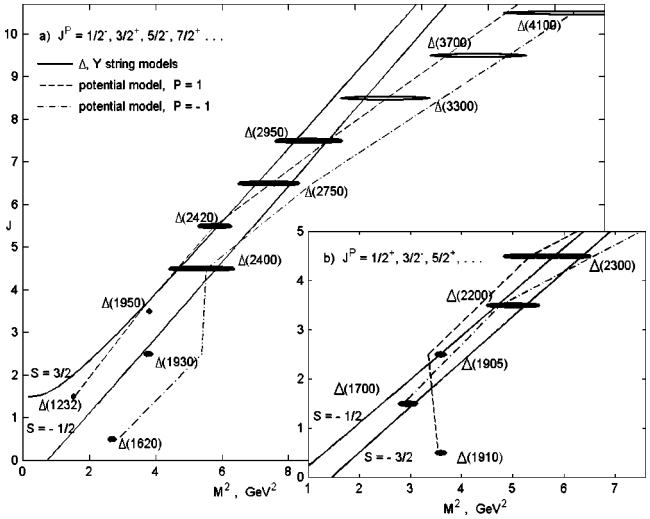

FIG. 5. RT for Δ baryons.

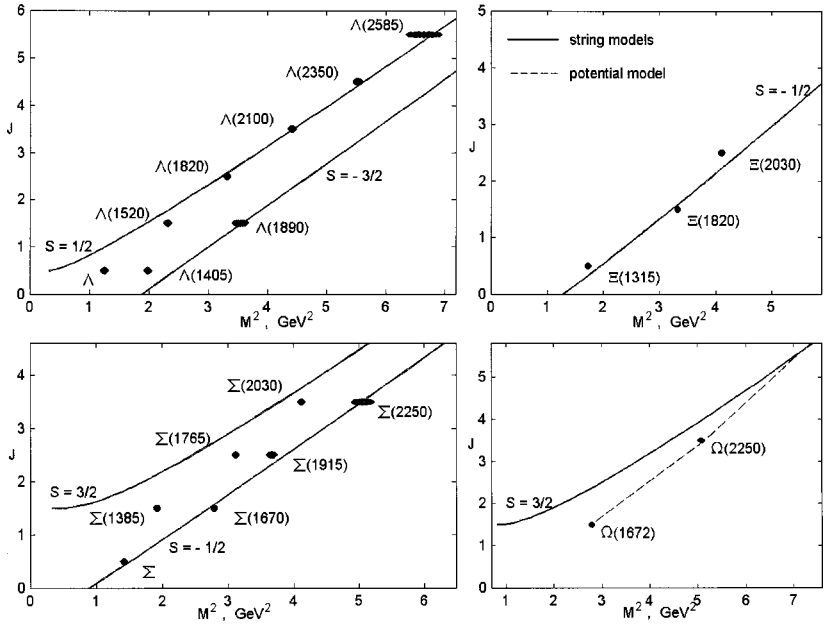

FIG. 6. RT for strange baryons.

parity are supposed to have $S=3/2$. In Fig. 4 the N-baryon states with $J^P=1/2^-$, $3/2^+$, $5/2^-$, . . . , are described by two different RT in the potential model [10] or by one RT with $S=1/2$ in the string models. Remember that the string models are not applicable to the states with small J or L. Otherwise, the potential model [10] is the most adequate for small L. It describes the strongly nonlinear RT generated by $N(1535)$ $1/2^-$ (Fig. 4) and $\Delta(1910)$ $1/2^+$ [Fig. 5(b)]. The string models do not predict such nonlinear behavior (convexity) at small J.

In Fig. 6 the results of the string models Δ and Y (q-qq is close to them) for the strange baryons Λ, Σ, and Ξ are represented. The potential model [10] predictions are calculated for Ω baryons. The string models are the most adequate for the particles, whose spin state may be interpreted as $S=\pm 1/2$ or for the RT with $S=3/2$ and with large J (Fig. 5).

In the charmed sector (Fig. 7) we know only a few states with $J=3/2$ and only one of them — $\Lambda_{c1}^+(2625)$ — may be interpreted as the orbital excitation of Λ_c^+. In Fig. 7 these particles are described by the q-qq, Y and Δ string configurations with the spin state $S=1/2$ and the summary spin of the light quarks $s_u+s_d=0$ (the upper curves in Fig. 7) similar to the strange Λ RT in Fig. 6. For the state Σ_c the trajectories with $S=-1/2$ and $s_u+s_d=-1$ are suggested.

For any string baryon model the corresponding meson-like model with the same (or corresponding) string tension, effective quark masses, types of spin correction must describe the RT in the meson sector. The results of this ''meson test'' for the string model [15] are represented in Fig. 8 for light and strange mesons in comparison with the results of the string meson model [14]. The latter model contains more fitting parameters (a set of a_n in addition to γ and m_i) so it describes some mesons better. But the results of the model [15] are satisfactory for the majority of light and strange meson states.

IV. DISCUSSION AND CONCLUSION

During the last two decades, a number of authors have shed some light on the problem of RT in the meson, baryon, and glueball sectors. Our approach in this paper is to analyze both *pure experimental* RT and predict properties of the RT in two different models: string and potential. This way we hope to understand better the fundamental property of RT — its linearity and when it is *broken*. In particular, our analysis of all available data from PDG98 [36] reveals that the following RT are essentially nonlinear (see Table V).

So, in total we have six baryon and ten meson experimental RT, which we consider as *essentially nonlinear*. We definitely witness the fundamental fact, that RT are not linear as a rule — it depends on intrinsic quark-gluon dynamics. One can observe nonlinearity for various RT in all current reso-

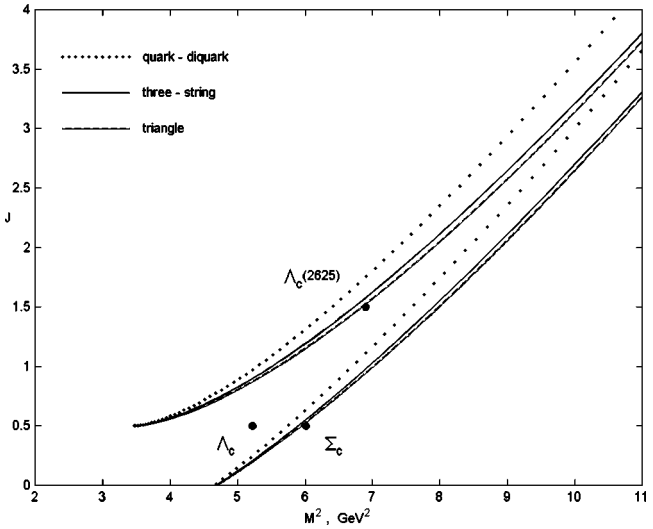

FIG. 7. RT for charmed baryons in string models.

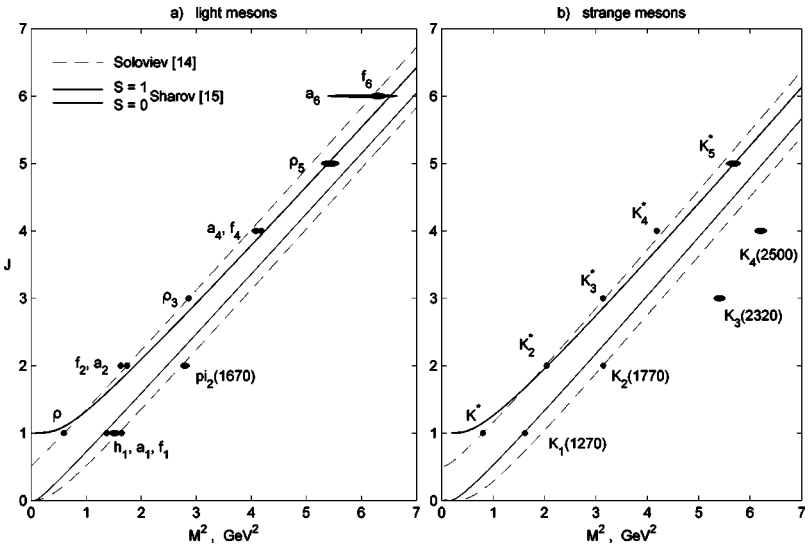

FIG. 8. RT for mesons in string models.

nance region — for low or large momenta.[3] Slopes for the experimental RT in Table V strongly differ from the standard $\alpha' \simeq 0.9$ GeV^{-2} and vary significantly along the given RT ($\sigma \sim 1$ GeV^{-2}).

Now we return to theoretical predictions and interpretations of RT for hadrons. In the series of papers [5], the authors introduced a new procedure for the solution of the SE for mesons, that is based on the expansion in the Planck constant $\hbar$. In contrast to a number of papers, which employed a WKB approximation, the authors of Ref. [5] assumed that their procedure will work for large as well as for small values N_r, and that this method is complementary to the WKB method. The authors of Ref. [5] investigated $\rho - a_2$, J/Ψ, and Υ parent and daughter RT and show that all usually employed potentials lead to nonlinear RT in the resonance region. However, they did not consider baryonic systems and did not show that the model adequately describes the *experimental* meson spectrum.

The authors of Ref. [3] investigated the baryon's RT in the relativistic approach, based on the method of vacuum correlators (MVC). Deriving the solutions of the dynamic equations the authors neglected the spin, isospin, Pauli principle, and one-gluon exchange potential, and thereby deduced that the RT were linear and found the N, Δ mass spectrum up to $K=6$. They found that slopes of baryonic and mesonic RT are equal ($\alpha' = 0.75$ GeV^{-2}). It is interesting that the authors compare these results with the previous paper of one of the authors (F.R.) [2], where the nonrelativistic SE with the power law confinement potential $r^{2/3}$ was used. The authors of Ref. [3] concluded that both methods gave very close spectra and linear RT. However, the above-cited authors [5] sharply criticized the paper [2] for misrepresenting the real picture in the resonance region, where the trajectories have a nonlinear character. Simonov lends support to our thesis in his collaboration with new authors; they very recently have noticed a *weak nonlinearity* of the mesonic RT [4] using MVC.

Dey *et al.* [6] described RT for mesons and baryons in q-deformed model and found a strong effect of nonlinearity for these RT, for rotational and radial excitations, including daughters. They study $\pi - b$, $\rho - a$, K, K^*, φ, $\omega - f$, Υ, Ψ meson families and N, Δ, Λ, Σ baryon families, computing spectra up to $J = 17/2$.

In his seminal paper [7] 't Hooft developed an $1/N_c$ relativistic, toy model for mesons, and he got a RT possessing some nonlinearity: ''... deviations from the straight line are expected near the origin as a consequence of the finiteness of the region of integration and the contribution of the mass

TABLE V. Slopes for nonlinear baryon, meson RT (α', average $\langle \alpha' \rangle$, mean square deviation σ in GeV^{-2}).

RT for baryons	slopes α' for neighbor pairs	$\langle \alpha' \rangle$	σ
N $3/2^-$ parent	0.80 1.02 0.702 0.45	0.74	0.20
Δ $1/2^+$ parent	3.53 1.20 0.40	1.71	1.33
N $1/2^-$ parent	4.44 0.89	2.67	1.78
N $1/2^-$ radial	2.73 0.61	1.67	1.06
N $3/2^-$ radial	1.72 0.70	1.21	0.51
Δ $1/2^-$ parent	1.82 0.98 1.11 0.60 0.34	0.97	0.51
RT for mesons	**slopes α'**	$\langle \alpha' \rangle$	σ
$f(0^{++})$ parent	3.00 0.78 0.94	1.58	1.01
$K(0^-)$ parent	0.73 1.14 0.34 1.25	0.87	0.36
$\rho - a_2$ parent	0.87 0.90 0.82 0.69 2.08	1.07	0.51
Υ radial	0.09 0.15 0.21 0.16 0.30	0.18	0.070
$\chi_b(1P)$ parent	1.58 2.37	1.97	0.40
$\chi_b(2P)$ parent	2.02 3.66	2.84	0.82
J/Ψ radial	0.25 1.60 2.11 1.03 0.46	1.09	0.69
f_0 radial	1.09 2.68 0.55 6.1 1.68	2.42	1.97
f_2 radial	2.39 2.48 4.27 1.64 1.82 4.95 1.9 1.42 5.13	2.88	1.39
$\chi_c(1P)$ parent	1.54 3.15	2.34	0.80

[3]But the data for the upper states with the largest J are not reliable in some cases [36].

terms $\cdots$.'' Mostly, the results of numerical analysis are described by the WKB mass formula with nonlinear logarithmic term.

We want to stress that few groups of authors simultaneously noted and discussed the nonlinearity of the experimental RT for J/Ψ and Υ families and its interplay with current theoretical quark models, namely Iachello [8], Semay [37], Stepanov [5], Dey [6], and Sergeenko [38]. Johnson *et al.* [39] used a semiclassical relativistic model for the orbital spectra of mesons, based on the assumption of a universal, flavor-independent linear confining interaction. They considered *yrast lines* for the families π, η, η', ρ, ω, K, K^*, φ, D, D^*, D_s, D_s^*, and, in particular, noted that π and K families do not lie on linear Chew-Frautschi plots. Johnson also found that the K^* family and ρ family have different slopes.

Durand *et al.* [40] also obtained varying slopes, describing spin-averaged spectra of strange, charmed and bottom mesons in the Bethe-Salpeter approach. Their range of variation for the slopes is very similar to that of the $\hbar$-expansion technique [5].

Iachello [41] analyzed parity doubling phenomena in the meson and baryon sectors. He has found out that parity doubling definitely takes place at low momenta, maximally pronounced at $J=5/2$, both experimentally and theoretically. Then, only at higher momenta linear RT appeared. It is marvelous, that our model [10] practically reproduces independently Figs. 10,11 from Ref. [41].

An attempt to describe analytically the quark-mass dependence in the meson RT for all flavors was made in Ref. [9] where the simple phenomenological model was built. The authors definitely got the gross feature of decreasing slope with increasing quark mass. The major drawback of Ref. [9] is that the authors did not account for J dependence of the slopes. In spite of this oversimplification, the trend of their results roughly resembled that of our Table III for median values $\langle \alpha' \rangle_i$.

Martin [1] also considered parent RT for mesons and baryons in the WKB approach and has derived simple *analytical* formulas for flavor-dependent slopes, which are decreasing with increasing quark mass. Martin's formulas are very different from the FPS [9], and he also noticed nonlinearity effects for RT in the resonance region.

Goldman and co-workers [42] used an unquenched lattice potential and computed the bottomonium spectrum. They demonstrated numerically that the effect of color screening is to produce *termination* of *nonlinear* hadronic parent and daughter's RT. These results are supported by recent lattice calculations, which observe *string breaking* [43]. It would be interesting to study the effect of color screening on light quarkonia and baryon's RT.

The results of our string and potential model fits and predictions for baryon and meson spectra and RT reveals distinctive feature — RT in many cases are *nonlinear* functions of J. This fundamental feature is in accord with analysis of *pure experimental* RT from PDG98 (Table V), and with predictions of different quark models, reviewed in this paper. Regge trajectories for mesons and baryons *are not* straight and parallel lines in general in the *current resonance region* both experimentally and theoretically, but *very often* have appreciable curvature, which is flavor-dependent. The effect of nonlinearity for a set of N and Δ baryon RT is described here in the frameworks of the considered potential model [10] (Figs. 3–5). This model predicts various forms of nonlinear behavior for the RT with various flavors (Figs. 1,2).

On the other hand, the string models of hadrons [14,15] with the standard action generate asymptotically linear RT with some form of nonlinearity at small J (only modifications of the action result in nonlinear RT). Nevertheless, on the basis of the considered string model [15] one can describe the majority of the light and strange RT for baryons and mesons (Figs. 3–8). The adequacy of this description is better for the most linear RT.

ACKNOWLEDGMENTS

A.I. is very grateful to G. Khaskin and Simon Fraser University, Burnaby, Canada for the help with computing facilities. G.S. is grateful for support by the Russian Foundation of Basic Research (grant 00-02-17359).

[1] A. Martin, Z. Phys. C **32**, 359 (1986).
[2] M. Fabre de la Ripelle, Phys. Lett. B **205**, 97 (1988).
[3] Y. Simonov and M. Fabre de la Ripelle, Ann. Phys. (N.Y.) **212**, 235 (1991).
[4] Y. Simonov, Phys. Lett. B **323**, 41 (1994); E. L. Gubankova and A. Y. Dubin, *ibid.* **334**, 180 (1994).
[5] F. Paccanoni, S. S. Stepanov, and R. S. Tutik, Mod. Phys. Lett. A **8**, 549 (1993); A. V. Kholodkov, F. Paccanoni, S. S. Stepanov, and R. S. Tutik, J. Phys. G **18**, 985 (1992); N. A. Kobylinsky, S. S. Stepanov, and R. S. Tutik, Z. Phys. C **47**, 469 (1990); Theor. Math. Phys. **90**, 208 (1992).
[6] J. Dey, P. Leal Ferreira, L. Tomio, and R. Roy Choudhury, Phys. Lett. B **331**, 355 (1994); J. Dey, M. Dey, P. L. Ferreira, and L. Tomio, *ibid.* **365**, 157 (1996).
[7] G. 't Hooft, Nucl. Phys. **B75**, 461 (1974).
[8] F. Iachello, N. C. Mukhopadhyay, and L. Zhang, Phys. Rev. D **44**, 898 (1991).
[9] S. Filipponi, G. Pancheri, and Y. Srivastava, Phys. Rev. Lett. **80**, 1838 (1998); S. Filipponi and Y. Srivastava, Phys. Rev. D **58**, 016003 (1998).
[10] A. Inopin and E. Inopin, Yad. Fiz. **53**, 562 (1991) [Sov. J. Nucl. Phys. **53**, 351 (1991)]; A. Inopin, A. Sinyugin, and E. Inopin, *Proceedings of the X International Seminar on High Energy Physics Problems* (World Scientific, Singapore, 1991); A. Inopin, πN Newsletter N13, ISSN 0942-4148, Proc. of MENU97, TRI-97-1, 221; A. Inopin and J. Swalby, Report No. APS1996SEP13-001; A. Inopin, Contributed paper No. 677 to ICHEP98, TRIUMF, Vancouver.
[11] A. Chodos and C. B. Thorn, Nucl. Phys. **B72**, 509 (1974); B. M. Barbashov and V. V. Nesterenko, Theor. Math. Phys. **31**, 465 (1977).

[12] Yu. I. Kobzarev, L. A. Kondratyuk, B. V. Martemyanov, and M. G. Shchepkin, Yad. Fiz. **45**, 526 (1987) [Sov. J. Nucl. Phys. **45**, 330 (1987)]; Yu. I. Kobzarev, B. V. Martemyanov, and M. G. Shchepkin, Usp. Fiz. Nauk. **162**(1), 1 (1992) [Sov. Phys. Usp. **35**, 257 (1992)].
[13] C. Olson, M. Olsson, and D. La Course, Phys. Rev. D **49**, 4675 (1994); D. La Course and M. Olsson, *ibid.* **39**, 2751 (1989); C. Goebel, La Course, and M. Olsson, *ibid.* **41**, 2917 (1990).
[14] L. D. Solov'ev, Theor. Math. Phys. **116**, 914 (1998); Phys. Rev. D **58**, 035005 (1998).
[15] G. S. Sharov, hep-ph/9809465; G. S. Sharov, Yad. Fiz. **62**, 1831 (1999) [Phys. At. Nucl. **62**, 1705 (1999)].
[16] K. Yamada, S. Ishida, J. Otokozawa, and N. Honzawa, Prog. Theor. Phys. **97**, 813 (1997).
[17] S. Gerasyuta, hep-ph/9810472.
[18] A. Hey and R. Kelly, Phys. Rep. **96**, 71 (1983).
[19] A. Hendry, in *Proceedings Baryon 80* (Isgur), p. 113; A. Hendry, Phys. Rev. Lett. **41**, 222 (1978).
[20] J. Richard and P. Taxil, Nucl. Phys. **B329**, 310 (1990); J. Richard, Phys. Rep. **212**, 1 (1992).
[21] R. Cutkosky and C. Forsyth, Z. Phys. C **18**, 219 (1983).
[22] A. Davydov and A. Chaban, Nucl. Phys. **20**, 499 (1960).
[23] B. M. Barbashov and V. V. Nesterenko, *Introduction to the Relativistic String Theory* (World Scientific, Singapore, 1990).
[24] Y. Nambu, Phys. Rev. D **10**, 4262 (1974).
[25] V. P. Petrov and G. S. Sharov, hep-ph/9812527.
[26] X. Artru, Nucl. Phys. **B85**, 442 (1975); K. Sundermeyer and A. de la Torre, Phys. Rev. D **15**, 1745 (1977).
[27] M. S. Plyushchay, G. P. Pronko, and A. V. Razumov, Theor. Math. Phys. **63**, 389 (1985); S. V. Klimenko *et al.*, *ibid.* **64**, 810 (1986).
[28] G. S. Sharov, Theor. Math. Phys. **113**, 1263 (1997).
[29] G. S. Sharov, Phys. Rev. D **58**, 114009 (1998).
[30] A. Inopin and G. S. Sharov, hep-ph/9905499.
[31] G. S. Sharov, Theor. Math. Phys. **114**, 220 (1998).
[32] G. S. Sharov and V. P. Petrov, hep-ph/9903429.
[33] T. J. Allen, M. C. Olsson, S. Veseli, and K. Williams, Phys. Rev. D **55**, 5408 (1997).
[34] B. M. Barbashov and G. S. Sharov, Theor. Math. Phys. **101**, 1332 (1994).
[35] G. S. Sharov, Theor. Math. Phys. **107**, 487 (1996); V. P. Petrov and G. S. Sharov, *ibid.* **109**, 1388 (1996).
[36] C. Caso *et al.*, Eur. Phys. J. C **3**, 1 (1998).
[37] C. Semay and R. Ceuleneer, Phys. Rev. D **48**, 4361 (1993).
[38] M. Sergeenko, Z. Phys. C **64**, 315 (1994).
[39] K. Johnson and C. Nohl, Phys. Rev. D **19**, 291 (1979).
[40] A. Gara, B. Durand, L. Durand, and L. J. Nickisch, Phys. Rev. D **40**, 843 (1989).
[41] F. Iachello, Nucl. Phys. **A497**, 23c (1989).
[42] M. M. Brisudova, L. Burakovsky, and T. Goldman, Phys. Lett. B **460**, 1 (1999).
[43] C. DeTar, O. Kaczmarek, F. Karsch, and E. Laermann, Phys. Rev. D **59**, 031501 (1999).